

Pion-nucleon scattering to $\mathcal{O}(p^4)$ in heavy baryon SU(3) chiral perturbation theory

Bo-Lin Huang ^{*1}

¹Department of Physics, Jishou University, Jishou 416000, China

January 19, 2022

Abstract

We calculate the T -matrices of pion-nucleon (πN) scattering to the fourth order in heavy baryon SU(3) chiral perturbation theory. The baryon mass in the chiral limit M_0 and the low-energy constants are determined by fitting to phase shifts of πN . By using these constants, we obtain an excellent description of S - and P -wave phase shifts below 200 MeV pion laboratory momentum. The scattering lengths and the scattering volumes are also predicted, which turn out to be in good agreement with those of other approaches and the available experimental data. Based on the various phase shifts and threshold parameters, the convergence of the chiral expansion is analyzed in detail. A good convergence in πN scattering is obtained at this order. In addition, we extend the fit to 250 MeV pion laboratory momentum, and obtain a good description of S - and P -wave phase shifts.

PACS numbers: 13.75.Jz, 12.39.Fe, 12.38.Bx

Keywords: Chiral perturbation theory, pion-nucleon scattering, chiral convergence

1 Introduction

Chiral perturbation theory (ChPT) allows one to analyze the low-energy hadronic processes, which is not accessible to a perturbative expansion in the strong coupling constant of quantum chromodynamics (QCD) [1, 2, 3, 4]. It is an efficient framework to calculate model-independent pion-nucleon (πN) scattering amplitude below the scale of chiral symmetry breaking $\Lambda_\chi \sim 1\text{ GeV}$. However, there exists a power-counting problem because of the nonzero baryon mass in the chiral limit M_0 . Over the years, several approaches to solve the power-counting problem have been proposed. The heavy baryon ChPT (HB χ PT) [5, 6], the infrared regularization (IR) baryon ChPT [7], and the extended-on-mass-shell (EOMS) baryon ChPT [8, 9] are the most popular approaches. The last two approaches are relativistic and have made substantial progress in many aspects [10, 11, 12, 13, 14, 15]. However, the expression from the loop diagrams in the relativistic approaches seems to become complicated [16, 17, 18]. The HB χ PT is a well-established and useful tool in the study of the low-energy hadronic processes. The expansion in HB χ PT is expanded simultaneously in terms of p/Λ_χ (non-relativistic terms) and p/M_0 (relativistic corrections), where p represents the meson momentum or its mass or the small residue momentum of a baryon in the non-relativistic limit.

In recent years, there has been a revival of interest in theoretical studies of elastic meson-baryon scattering at low energy. It is concerned not merely with the understanding of the strong interaction, but with the properties of single and multi baryons. The low-energy processes of pions and nucleons are widely investigated in the SU(2) HB χ PT [19, 20, 21, 22]. For processes involving kaons or hyperons, the situation is more complicated. One has to use three-flavor chiral dynamics. In a previous paper [23] we investigated the KN and $\bar{K}N$ elastic scattering to one-loop order in SU(3) HB χ PT by fitting to partial-wave phase shifts of KN scattering and obtained reasonable results. Then, we extended this approach to predictions for pseudoscalar meson octet-baryon scattering in all channels by fitting to partial-wave phase shifts of πN and KN scattering [24]. Note that the predictions for the meson-baryon scattering lengths in SU(3) HB χ PT have been given in detail [25, 26, 27, 28, 29]. However, our study has been extended to

*bolin.huang@foxmail.com

partial-wave phase shifts, pion-nucleon sigma terms, etc. That can allow us not only to obtain much more information of hadron but also to get a better understanding of ChPT. In the last paper [30], we calculated the complete T matrices of pion-nucleon scattering to the third order in SU(3) HB χ PT. We obtained some properties of baryon, e.g., pion-nucleon sigma term $\sigma_{\pi N}$. A good description for the phase shifts of πN scattering below 200 MeV was also obtained. It can be a consistency check to consider the other meson-baryon scattering. Nevertheless, a good convergence has not been received for chiral expansions up to third order. In this paper, we will calculate the T matrices for πN scattering to fourth order in SU(3) HB χ PT. The M_0 and the low-energy constants (LECs) will be determined by fitting to phase shifts of πN . In particular, the dimension two LECs will be obtained separately. The convergence of the chiral expansions will be discussed in detail. In addition, the chiral expansions should be more accurate with the increase of the chiral order, the description of πN phase shifts at higher energies will be presented.

In Sec. 2, we summarize the Lagrangians involved in the evaluation up to the fourth-order contributions. In Sec. 3, we present the T matrices of the elastic πN scattering. In Sec. 4, we outline how to calculate phase shifts, scattering lengths, and scattering volumes. Section 5 contains the results and discussions and also includes a brief summary.

2 Chiral Lagrangian

In order to calculate the pion-nucleon scattering amplitudes up to order $\mathcal{O}(p^4)$ in heavy baryon SU(3) chiral perturbation theory, the corresponding effective Lagrangian can be written as

$$\mathcal{L}_{\text{eff}} = \mathcal{L}_{\phi\phi}^{(2)} + \mathcal{L}_{\phi B}^{(1)} + \mathcal{L}_{\phi B}^{(2)} + \mathcal{L}_{\phi B}^{(3)} + \mathcal{L}_{\phi B}^{(4)}. \quad (1)$$

The traceless Hermitian 3×3 matrices ϕ and B include the pseudoscalar Goldstone boson fields (π, K, \bar{K}, η) and the octet-baryon fields (N, Λ, Σ, Ξ), respectively. The explicit form of the $\mathcal{L}_{\phi\phi}^{(2)}$, $\mathcal{L}_{\phi B}^{(1)}$, $\mathcal{L}_{\phi B}^{(2)}$ and $\mathcal{L}_{\phi B}^{(3)}$ can be found in Ref. [30]. The complete fourth-order heavy baryon Lagrangian $\mathcal{L}_{\phi B}^{(4)}$ obviously splits up into two parts, relativistic corrections with fixed coefficients and counterterms proportional to the low-energy constants. The relativistic terms can be obtained from the original relativistic leading-order, next-to-leading-order and next-to-next-to-leading-order Lagrangian in terms of path integrals [6]. The dimension four three-flavor Lorentz-invariant meson-baryon chiral Lagrangian has been constructed in Ref. [31]. We can obtain the counter-term Lagrangian from the relativistic effective meson-baryon chiral Lagrangian. However, the dimension four Lagrangian is tedious, the explicit expressions are not given. In fact, it is not necessary to give the explicit expressions since we only consider pion-nucleon scattering. The various expansions from tree diagrams in SU(3) and SU(2) HB χ PT are consistent. For the dimension four counterterms, the low-energy constants \bar{e}_i ($i = 14, \dots, 22, 35, \dots, 38$) in SU(2) HB χ PT from Ref. [20] are also used in this paper.

3 T -matrices for pion-nucleon scattering

We are considering only elastic pion-nucleon scattering processes $\pi(q) + N(p) \rightarrow \pi(q') + N(p')$ in the center-of-mass system (CMS). In the total isospin $I = (1/2, 3/2)$ of the pion-nucleon system, the corresponding T -matrix takes the following form:

$$T_{\pi N}^{(I)} = V_{\pi N}^{(I)}(w, t) + i\boldsymbol{\sigma} \cdot (\mathbf{q}' \times \mathbf{q}) W_{\pi N}^{(I)}(w, t) \quad (2)$$

where $w = v \cdot q = v \cdot q' = (m_\pi^2 + \mathbf{q}^2)^{1/2}$ is the pion CMS energy, $t = (q' - q)^2 = 2\mathbf{q}^2(z - 1)$ is the invariant momentum transfer squared with $z = \cos(\theta)$ the cosine of the angle θ between \mathbf{q} and \mathbf{q}' . Based upon relativistic kinematics, we have

$$\mathbf{q}'^2 = \mathbf{q}^2 = \frac{M_N^2 \mathbf{p}_{\text{lab}}^2}{m_\pi^2 + M_N^2 + 2M_N \sqrt{m_\pi^2 + \mathbf{p}_{\text{lab}}^2}}, \quad (3)$$

where \mathbf{p}_{lab} denotes the momentum of the incident meson in the laboratory system. Furthermore, $V_{\pi N}^{(I)}(w, t)$ refers to the non-spin-flip pion-nucleon amplitude and $W_{\pi N}^{(I)}(w, t)$ refers to the spin-flip pion-nucleon amplitude.

From the leading-order $\mathcal{O}(q)$ to the third order $\mathcal{O}(q^3)$, the amplitudes can be found in Ref. [30]. At fourth order $\mathcal{O}(q^4)$, for the amplitudes from tree diagrams, the results are consistent with the amplitudes calculated in the SU(2) HB χ PT. For a more detailed calculation, we refer to Ref. [20]. After the appropriate replacement of the constants, the amplitudes read

$$\begin{aligned}
V_{\pi N}^{(3/2, \text{N3LO})} = & -\frac{(D+F)^2}{32M_0^3 w^4 f_\pi^2} [(t^4 + 7t^3 w^2 + 11t^2 w^4 - 3tw^6 + 4w^8) - (11t^3 + 49t^2 w^2 + 32tw^4 \\
& + 4w^6)m_\pi^2 + (45t^2 + 110tw^2 + 26w^4)m_\pi^4 - 3(27t + 26w^2)m_\pi^6 + 54m_\pi^8] \\
& + \frac{m_\pi^2 - w^2}{32M_0^3 f_\pi^2} (4m_\pi^2 - t - 4w^2) + \frac{1}{16M_0^2 f_\pi^2} [4C_0(t + 2w^2 - 2m_\pi^2)m_\pi^2 + C_1(2t^2 + 4tw^2 \\
& - 8tm_\pi^2 - 8w^2 m_\pi^2 + 8m_\pi^4) + 4C_2(3tw^2 + 14w^4 - 4tm_\pi^2 - 22w^2 m_\pi^2 + 8m_\pi^4) \\
& + 2C_3(-t^2 - 4tw^2 + 4tm_\pi^2)] - \frac{8}{M_0 f_\pi^2} C_0 C_2 w^2 m_\pi^2 + \frac{1}{2M_0 f_\pi^2} [H_1(4m_\pi^2 - t - 4w^2)m_\pi^2 \\
& + H_2(4w^2 + t - 4m_\pi^2)t + 3H_3(4m_\pi^2 - t - 4w^2)w^2 + 2H_4 w^2 t] \\
& + \frac{1}{f_\pi^2} [4\bar{e}_{14}(4m_\pi^4 - 4m_\pi^2 t - t^2) + 8\bar{e}_{15}(2w^2 m_\pi^2 - tw^2) + 16\bar{e}_{16} w^4], \tag{4}
\end{aligned}$$

$$\begin{aligned}
W_{\pi N}^{(3/2, \text{N3LO})} = & \frac{(D+F)^2}{16M_0^3 w^4 f_\pi^2} [(t^3 + 5t^2 w^2 + 3tw^4 - w^6) - (9t^2 + 25tw^2 + 4w^4)m_\pi^2 \\
& + 3(9t + 10w^2)m_\pi^4 - 27m_\pi^6] + \frac{w^2 - m_\pi^2}{16M_0^3 f_\pi^2} + \frac{1}{8M_0^2 f_\pi^2} [8C_0 m_\pi^2 + C_1(2t - 4m_\pi^2) \\
& - 4C_2 w^2 - 2C_3(t + 2w^2 - 2m_\pi^2)] + \frac{1}{2M_0 f_\pi^2} H_4(8w^2 + t - 4m_\pi^2) \\
& + \frac{1}{f_\pi^2} [\bar{e}_{17}(-8m_\pi^2 + 4t) - 8\bar{e}_{18} w^2], \tag{5}
\end{aligned}$$

$$\begin{aligned}
V_{\pi N}^{(1/2, \text{N3LO})} = & \frac{(D+F)^2}{64M_0^3 w^4 f_\pi^2} [(t^4 + 7t^3 w^2 + 11t^2 w^4 + 16w^8) - (11t^3 + 49t^2 w^2 + 32tw^4 \\
& + 16w^6)m_\pi^2 + 5(9t^2 + 22tw^2 + 4w^4)m_\pi^4 - 84(t + w^2)m_\pi^6 + 60m_\pi^8] \\
& + \frac{w^2 - m_\pi^2}{16M_0^3 f_\pi^2} (4m_\pi^2 - t - 4w^2) + \frac{1}{8M_0^2 f_\pi^2} [2C_0(t + 2w^2 - 2m_\pi^2)m_\pi^2 + C_1(t^2 + 2tw^2 \\
& - 4tm_\pi^2 - 4w^2 m_\pi^2 + 4m_\pi^4) + 2C_2(3tw^2 + 14w^4 - 4tm_\pi^2 - 22w^2 m_\pi^2 + 8m_\pi^4) \\
& + 2C_3(t^2 + 4tw^2 - 4tm_\pi^2)] - \frac{8}{M_0 f_\pi^2} C_0 C_2 w^2 m_\pi^2 + \frac{1}{M_0 f_\pi^2} [H_1(-4m_\pi^2 + t + 4w^2)m_\pi^2 \\
& - H_2(4w^2 + t - 4m_\pi^2)t - 3H_3(4m_\pi^2 - t - 4w^2)w^2 + H_4 w^2 t] \\
& + \frac{1}{f_\pi^2} [4\bar{e}_{14}(4m_\pi^4 - 4m_\pi^2 t - t^2) + 8\bar{e}_{15}(2w^2 m_\pi^2 - tw^2) + 16\bar{e}_{16} w^4], \tag{6}
\end{aligned}$$

$$\begin{aligned}
W_{\pi N}^{(1/2, \text{N3LO})} = & \frac{(D+F)^2}{32M_0^3 w^4 f_\pi^2} [(-t^3 - 5t^2 w^2 - 3tw^4 + 4w^6) + (9t^2 + 25tw^2 + 4w^4)m_\pi^2 \\
& - 3(9t + 10w^2)m_\pi^4 + 24m_\pi^6] + \frac{m_\pi^2 - w^2}{8M_0^3 f_\pi^2} + \frac{1}{4M_0^2 f_\pi^2} [-2C_0 m_\pi^2 + C_1(t - 2m_\pi^2) \\
& - 2C_2 w^2 + 2C_3(t + 2w^2 - 2m_\pi^2)] + \frac{1}{2M_0 f_\pi^2} H_4(8w^2 + t - 4m_\pi^2) \\
& + \frac{8}{f_\pi^2} [\bar{e}_{17}(2m_\pi^2 - t) + 2\bar{e}_{18} w^2], \tag{7}
\end{aligned}$$

where $C_i (i = 0, \dots, 3)$ and $H_i (i = 1, \dots, 4)$ are from the Eq. (22) and Eq. (27) of the Ref. [30], respectively. For the dimension four LECs, we take the same strategy as the dimension four LECs $\bar{e}_i (i = 19, \dots, 22, 35, \dots, 38)$ were absorbed into the dimension two LECs $c_i (i = 1, \dots, 4)$, see Eq. (3.23) of the Ref. [20]. Note that, the dimension two LECs $c_i (i = 1, \dots, 4)$ from SU(2) HB χ PT can be replaced with the combinations of the LECs $C_i (i = 0, \dots, 3)$ from SU(3) HB χ PT. Thus, $\bar{e}_i (i = 14, \dots, 18)$ are the remaining dimension four LECs in our calculation. At this order,

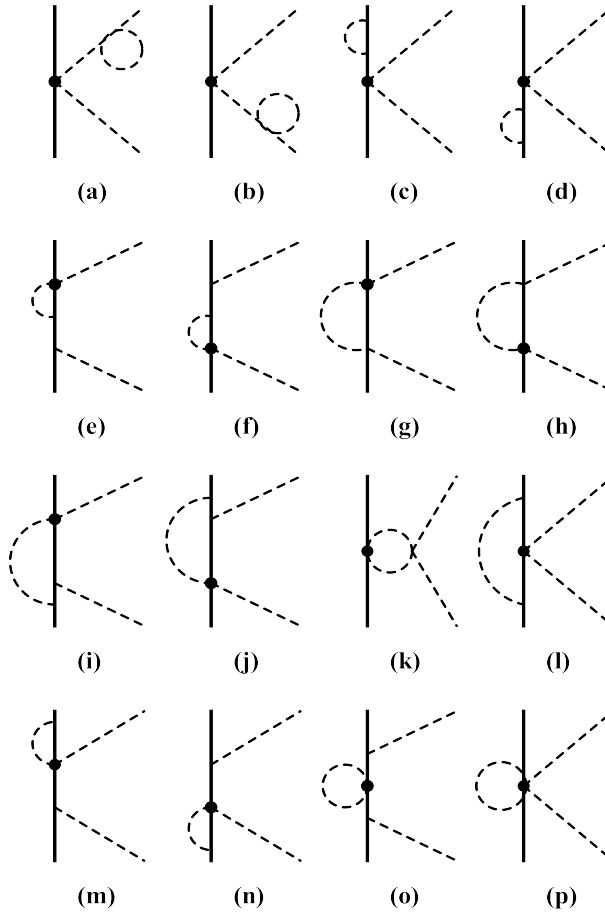


Figure 1: Nonvanishing one-loop diagrams contributing at fourth chiral order. The heavy dots refer to vertices from $\mathcal{L}_{\phi B}^{(2)}$. Crossed graphs are not shown.

the amplitudes from one-loop diagrams should also be considered. The nonvanishing one-loop diagrams generated by the vertices of $\mathcal{L}_{\phi\phi}^{(2)}$, $\mathcal{L}_{\phi B}^{(1)}$ and $\mathcal{L}_{\phi B}^{(2)}$ are shown in Figure 1. The one-loop amplitudes are tedious, the explicit analytical expression for the loop contributions of the order $\mathcal{O}(q^4)$ to the pion-nucleon scattering can be obtained from the author upon request. Note that, the one-loop amplitudes of the order $\mathcal{O}(q^4)$ contain the dimension two LECs b_i ($i = D, F, 0, \dots, 11$), they can not be combined into the combinations of the LECs C_i ($i = 0, \dots, 3$). Thus, the dimension two LECs b_i ($i = D, F, 0, \dots, 11$) are used directly in final amplitudes.

4 Calculating phase shifts and scattering lengths

The partial-wave amplitudes $f_j^{(I)}(\mathbf{q}^2)$, where $j = l \pm 1/2$ refers to the total angular momentum and l to orbital angular momentum, are obtained from the non-spin-flip and spin-flip amplitudes by a projection:

$$f_{l\pm 1/2}^{(I)}(\mathbf{q}^2) = \frac{M_N}{8\pi(w+E)} \int_{-1}^{+1} dz \left\{ V_{\pi N}^{(I)} P_l(z) + \mathbf{q}^2 W_{\pi N}^{(I)} [P_{l\pm 1}(z) - zP_l(z)] \right\}, \quad (8)$$

where $P_l(z)$ denotes the conventional Legendre polynomial, and $w+E = \sqrt{m_\pi^2 + \mathbf{q}^2} + \sqrt{M_N^2 + \mathbf{q}^2}$ is the total center-of-mass energy. For the energy range considered in this paper, the phase shifts $\delta_{l\pm 1/2}^{(I)}$ are calculated by (also see Refs. [19, 32])

$$\delta_{l\pm 1/2}^{(I)} = \arctan[|\mathbf{q}| \operatorname{Re} f_{l\pm 1/2}^{(I)}(\mathbf{q}^2)]. \quad (9)$$

The scattering lengths for s waves and the scattering volumes for p waves are obtained by approaching the threshold [33]

$$a_{l\pm 1/2}^{(I)} = \lim_{|\mathbf{q}| \rightarrow 0} \mathbf{q}^{-2l} f_{l\pm 1/2}^{(I)}(\mathbf{q}^2). \quad (10)$$

5 Results and discussion

Before presenting results, we have to determine the M_0 and the LECs. Unfortunately, the 14 dimension-two LECs can not be regrouped up to fourth order in SU(3) HB χ PT. Then, in total, there are 24 unknown constants that need to be determined. Throughout this paper, we also use $m_\pi = 139.57$ MeV, $m_K = 493.68$ MeV, $m_\eta = 547.86$ MeV, $f_\pi = 92.07$ MeV, $f_K = 110.03$ MeV, $f_\eta = 1.2f_\pi$, $M_N = 938.92 \pm 1.29$ MeV, $M_\Sigma = 1191.01 \pm 4.86$ MeV, $M_\Xi = 1318.26 \pm 6.30$ MeV, $M_\Lambda = 1115.68 \pm 5.58$ MeV, $\lambda = 4\pi f_\pi = 1.16$ GeV, $D = 0.80$ and $F = 0.47$ [34, 35, 36].

We have various fitting strategies to determine the pertinent constants, the related discussion

Table 1: Values of the various fits. The fit 1, 2, 3 refer to the best fit up to fourth, third and second order, respectively. For a detailed description of these fits, see the main text. Note that the (*) values are calculated by b_i .

	Fit 1	Fit 2	Fit 3
M_0 (MeV)	370.56 ± 74.11	1530.20 ± 290.87	373.47 ± 27.65
b_D (GeV $^{-1}$)	-0.18 ± 0.03		
b_F (GeV $^{-1}$)	0.96 ± 0.19		
b_0 (GeV $^{-1}$)	-1.47 ± 0.29		
b_1 (GeV $^{-1}$)	-0.31 ± 0.06		
b_2 (GeV $^{-1}$)	0.12 ± 0.02		
b_3 (GeV $^{-1}$)	-9.24 ± 0.92		
b_4 (GeV $^{-1}$)	3.95 ± 0.39		
b_5 (GeV $^{-1}$)	-11.12 ± 0.56		
b_6 (GeV $^{-1}$)	0.57 ± 0.11		
b_7 (GeV $^{-1}$)	4.77 ± 0.95		
b_8 (GeV $^{-1}$)	1.35 ± 0.27		
b_9 (GeV $^{-1}$)	-2.14 ± 0.43		
b_{10} (GeV $^{-1}$)	-0.33 ± 0.00		
b_{11} (GeV $^{-1}$)	-5.94 ± 0.59		
C_0 (GeV $^{-1}$)	$-2.14 \pm 0.61^{(*)}$	-3.19 ± 0.23	-2.17 ± 0.82
C_1 (GeV $^{-1}$)	$-6.75 \pm 0.14^{(*)}$	-7.39 ± 0.10	-4.49 ± 0.12
C_2 (GeV $^{-1}$)	$-18.66 \pm 1.84^{(*)}$	4.81 ± 0.22	2.87 ± 0.67
C_3 (GeV $^{-1}$)	$-1.08 \pm 1.98^{(*)}$	1.72 ± 0.04	1.18 ± 0.02
H_1 (GeV $^{-2}$)	31.79 ± 6.36	8.77 ± 0.95	
H_2 (GeV $^{-2}$)	5.25 ± 0.53	5.17 ± 0.16	
H_3 (GeV $^{-2}$)	-8.69 ± 0.43	-10.25 ± 0.71	
H_4 (GeV $^{-2}$)	-15.91 ± 0.79	-8.33 ± 0.31	
\bar{e}_{14} (GeV $^{-3}$)	28.64 ± 1.43		
\bar{e}_{15} (GeV $^{-3}$)	25.22 ± 5.04		
\bar{e}_{16} (GeV $^{-3}$)	4.59 ± 0.92		
\bar{e}_{17} (GeV $^{-3}$)	5.61 ± 1.12		
\bar{e}_{18} (GeV $^{-3}$)	5.61 ± 1.12		
$\chi^2/\text{d.o.f.}$	0.62	1.63	4.12

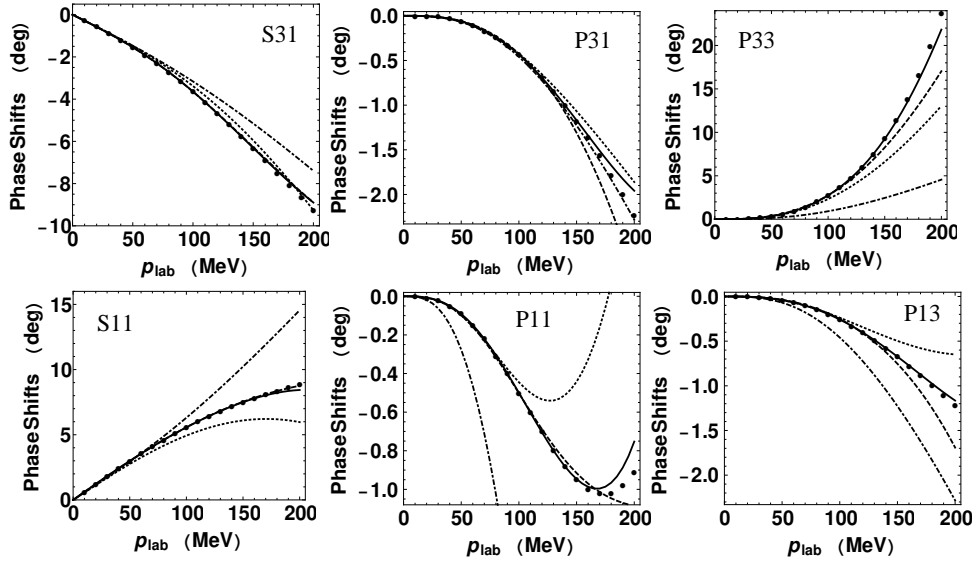


Figure 2: Fits and predictions for the WI08 phase shifts versus the pion lab. momentum $|\mathbf{p}_{\text{lab}}|$ in pion-nucleon (πN) scattering. The dot-dashed, dotted, dashed and solid lines refer to the best fits up to first, second, third and fourth order, respectively. Fitting for all πN waves are the data in the range of 50-150 MeV. For higher and lower energies, the phase shifts are predicted.

is given in Ref. [30]. One of them is using the octet-baryon masses ($M_{N,\Sigma,\Xi,\Lambda}$) and the phase shifts of πN scattering simultaneously, this can no longer be done up to fourth order due to the appearance of the more constants for octet-baryon masses. Thus, we determine the M_0 and LECs by using the phase shifts of the WI08 solution [37, 38] for πN scattering directly. We choose a common uncertainty of $\pm 2\%$ to all phase shifts before the fitting procedure. The data points of the S and P waves in the range of 50-150 MeV pion lab. momentum are used. Therefore, there are 66 data in total for this fitting. The resulting M_0 and LECs can be found in Fit 1 of Table 1. The uncertainty for the respective parameter is purely estimated (for a detailed discussion, see, e.g., Refs.[39, 40]). It is not surprise that most of LECs are natural size, i.e. the absolute values of these LECs are between one and ten when one introduces the dimensionless LECs (e.g., $b'_i = 2M_0 b_i$), whereas some of LECs come out fairly large. The situation also can be found in SU(2) HB χ PT [20]. We can also find that the baryon mass in the chiral limit M_0 appears small. It is smaller than any physical value of the octet-baryon mass. However, the M_0 value is reasonable because it is a non-physical quantity. The corresponding S - and P -wave phase shifts are shown by the solid lines of Fig. 2. Obviously, we obtain an excellent description of all waves. Especially, the description of the $P33$ -, and $P13$ -wave phase shifts are improved at high energies as compared to the third-order calculation. For comparison, we present results from the best fits up to third (fit 2) and second (fit 3) order in Table 1. Clearly, the resulting M_0 and LECs have different values in the respective order. Thus, for the amplitudes up to the

Table 2: Values of the S - and P -wave scattering lengths and scattering volumes in comparison with the values of the various analyses.

	Our results	SU(2) [20]	SP98 [20]	EXP2001 [41]	EXP2015 [42]
$a_{0+}^{3/2}$ (fm)	-0.114 ± 0.003	-0.119	-0.125 ± 0.002	-0.125 ± 0.003	-0.122 ± 0.003
$a_{0+}^{1/2}$ (fm)	0.243 ± 0.002	0.249	0.250 ± 0.002	$0.250^{+0.006}_{-0.004}$	0.240 ± 0.003
$a_{1+}^{3/2}$ (fm ³)	0.589 ± 0.021	0.586	0.595 ± 0.005
$a_{1+}^{1/2}$ (fm ³)	-0.072 ± 0.004	-0.054	-0.038 ± 0.008
$a_{1-}^{3/2}$ (fm ³)	-0.108 ± 0.012	-0.113	-0.122 ± 0.006
$a_{1-}^{1/2}$ (fm ³)	-0.171 ± 0.010	-0.181	-0.207 ± 0.007

Table 3: Values of the S - and P -wave scattering lengths and scattering volumes from the different order.

	$\mathcal{O}(q)$	$\mathcal{O}(q^2)$	$\mathcal{O}(q^3)$	$\mathcal{O}(q^4)$
$a_{0+}^{3/2}$ (fm)	-0.113	-0.112 ± 0.067	-0.132 ± 0.042	-0.114 ± 0.003
$a_{0+}^{1/2}$ (fm)	0.225	0.226 ± 0.067	0.214 ± 0.066	0.243 ± 0.002
$a_{1+}^{3/2}$ (fm ³)	0.241	0.569 ± 0.008	0.617 ± 0.014	0.589 ± 0.021
$a_{1+}^{1/2}$ (fm ³)	-0.121	-0.077 ± 0.006	-0.070 ± 0.010	-0.072 ± 0.004
$a_{1-}^{3/2}$ (fm ³)	-0.121	-0.119 ± 0.008	-0.108 ± 0.012	-0.108 ± 0.012
$a_{1-}^{1/2}$ (fm ³)	-0.483	-0.194 ± 0.009	-0.192 ± 0.018	-0.171 ± 0.010

given order, the corresponding fit to determine their respective constants is necessary.

In the following, let us apply the chiral fourth order amplitudes to estimate the threshold parameters. Since we do not fit data below 50 MeV, the pion-nucleon scattering lengths and scattering volumes are now predictions. The threshold parameters are obtained by using an incident pion lab. momentum $|\mathbf{p}_{\text{lab}}| = 10\text{MeV}$ and approximating their values at the threshold. The results are shown in Table 2 in comparison with the values of the various analyses. Obviously, our results for both scattering lengths and scattering volumes are consistent with the ones from SU(2) HB χ PT [20]. The description for the other results can be found in Ref. [30]. As expected, our results for the threshold parameters are consistent with those values within errors.

Next, we can discuss the convergence of the chiral expansion. In Fig. 2, we show the best fits up to the respective order. In all partial-waves, the fourth-order corrections are smaller than the third-order ones, indicating convergence. In most cases, the third-order corrections are smaller than the second-order ones. The second-order corrections are smaller than the first-order ones in a few partial-waves. Therefore, the convergence of the chiral expansion becomes better along with the increase of the order. However, with the energy increasing the convergence of the chiral expansion becomes worse. The fact is not surprise because the chiral expansion is expanded in terms of p/Λ_χ . We can also study the convergence of the threshold parameters, see Table 3. The two scattering lengths $a_{0+}^{3/2}$ and $a_{0+}^{1/2}$ from S waves are almost unchanged in different order, indicating convergence in each order. The other four scattering volumes from P waves are consistent from order $\mathcal{O}(q^2)$. The calculation results indicate the convergence of the threshold parameters is fast that is due to $m_\pi/\Lambda_\chi \sim 1/7$. To sum up, we obtain a good convergence in πN scattering.

Table 4: Values of the fit in the range of 50-250MeV at fourth order.

M_0 (MeV)	512.66 ± 102.53	b_9 (GeV ⁻¹)	0.85 ± 0.04
b_D (GeV ⁻¹)	1.80 ± 0.09	b_{10} (GeV ⁻¹)	-1.93 ± 0.08
b_F (GeV ⁻¹)	-1.85 ± 0.09	b_{11} (GeV ⁻¹)	0.45 ± 0.01
b_0 (GeV ⁻¹)	1.46 ± 0.07	H_1 (GeV ⁻²)	46.14 ± 2.31
b_1 (GeV ⁻¹)	-0.92 ± 0.05	H_2 (GeV ⁻²)	10.53 ± 0.53
b_2 (GeV ⁻¹)	-3.00 ± 0.15	H_3 (GeV ⁻²)	-11.22 ± 0.56
b_3 (GeV ⁻¹)	0.06 ± 0.00	H_4 (GeV ⁻²)	-15.65 ± 0.78
b_4 (GeV ⁻¹)	4.05 ± 0.29	\bar{e}_{14} (GeV ⁻³)	6.41 ± 0.33
b_5 (GeV ⁻¹)	-13.04 ± 0.66	\bar{e}_{15} (GeV ⁻³)	-8.42 ± 0.45
b_6 (GeV ⁻¹)	0.23 ± 0.01	\bar{e}_{16} (GeV ⁻³)	8.77 ± 0.44
b_7 (GeV ⁻¹)	8.60 ± 0.45	\bar{e}_{17} (GeV ⁻³)	5.22 ± 0.26
b_8 (GeV ⁻¹)	1.55 ± 0.28	\bar{e}_{18} (GeV ⁻³)	5.22 ± 0.26

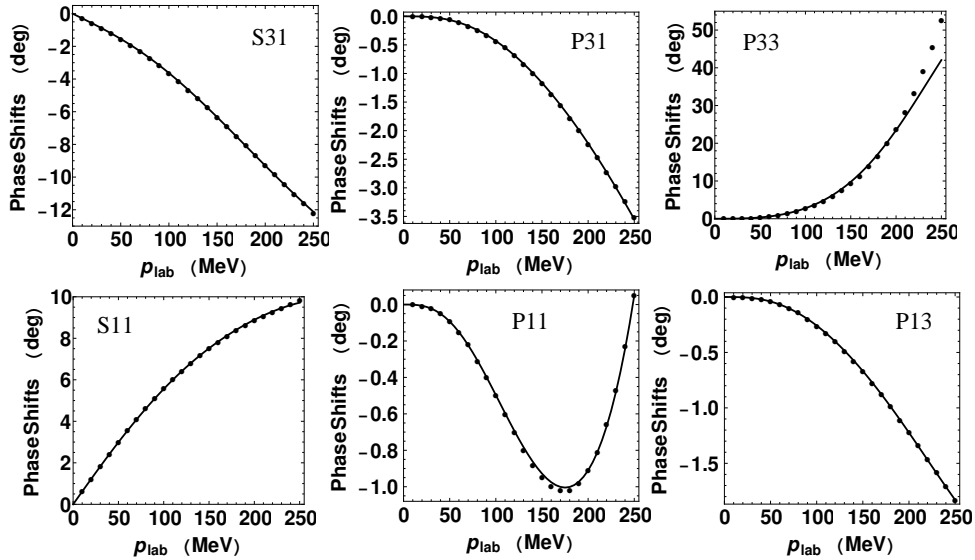


Figure 3: Fits for the WI08 phase shifts versus the pion lab. momentum $|\mathbf{p}_{\text{lab}}|$ in pion-nucleon (πN) scattering at fourth order. Fitting for all πN waves are the data in the range of 50-250 MeV.

Based on the excellent description of all waves and the good convergence at fourth order, now we extend the fit to 250 MeV pion lab. momentum (corresponding to a energy in CMS of $\sqrt{s} \sim 1.2$ GeV). We also choose a common uncertainty of $\pm 2\%$ to all phase shifts. The data points of the S and P waves in the range of the 50-250 MeV pion lab. momentum are used. Thus, there are 126 data in total for this fitting. The resulting M_0 and LECs are shown in Table 4. We obtain a large $\chi^2/\text{d.o.f.} \simeq 3.15$ because we choose a small common uncertainty to all phase shifts. The value of the baryon mass in the chiral limit M_0 is more close to the physical value and seems more reasonable. The values of the LECs are also different from the values which are obtained by fitting in range of 50-150 MeV pion lab. momentum, see Table 1. The corresponding S - and P -wave phase shifts are shown in Fig. 3. This time, we obtain a good description of all waves except for the $P33$ -wave at high energy. That is due to the exist of the resonance $\Delta(1232)$ in $P33$ -wave. A good description of the $P33$ -wave up to 250 MeV was obtained when the lowest order decuplet contributions were included in Ref. [18]. Thus, for the description of πN phase shifts at high energies, the other hadronic contributions can not be ignored.

In summary, we calculated the T matrices for pion-nucleon scattering to the fourth order in SU(3) HB χ PT. We fitted the WI08 phase shifts of πN scattering in range of 50-150 MeV pion lab. momentum to determine the M_0 and the LECs. This led to a excellent description of S - and P -wave phase shifts below 200 MeV pion lab. momentum. The scattering lengths and scattering volumes were also calculated at this order, which turned out to be in good agreement with those of the approaches and available experimental data. We discussed the convergence of the chiral expansion based on the phase shifts and threshold parameters from the best fits up to the respective order in detail. To sum up, we obtained a good convergence in πN scattering at this order. Finally, we extended the description for phase shifts of πN scattering to 250 MeV pion lab. momentum. The reasonable M_0 and LECS are also obtained. They may can be used for the other physical processes as input. A good description of all waves except for the $P33$ -wave at high energy were obtained. An improved results for πN scattering may be to achieve through including the resonance $\Delta(1232)$ and the other hadronic contributions.

Acknowledgments

This work is supported by the National Natural Science Foundation of China under Grant No. 11947036. I thank Norbert Kaiser (Technische Universität München), Yan-Rui Liu (Shandong University), Li-Sheng Geng (Beihang University), Jun-Xu Lu (Beihang University) and Jing Ou-Yang (Jishou University) for very helpful discussions.

References

- [1] S. Weinberg. Phenomenological Lagrangians. *Physica A*, 96:327–340, 1979.
- [2] J. Gasser and H. Leutwyler. Chiral perturbation theory to one loop. *Annals Phys.*, 158:142, 1984.
- [3] H. Leutwyler. On the foundations of chiral perturbation theory. *Annals Phys.*, 235:165–203, 1994.
- [4] S. Scherer and M. R. Schindler. A primer for chiral perturbation theory. *Lect. Notes Phys.*, 830:pp.1–338, 2012.
- [5] E. E. Jenkins and A. V. Manohar. Baryon chiral perturbation theory using a heavy fermion Lagrangian. *Phys. Lett. B*, 255:558–562, 1991.
- [6] V. Bernard, N. Kaiser, J. Kambor, and U.-G. Meißner. Chiral structure of the nucleon. *Nucl. Phys. B*, 388:315–345, 1992.
- [7] T. Becher and H. Leutwyler. Baryon chiral perturbation theory in manifestly Lorentz invariant form. *Eur. Phys. J. C*, 9:643–671, 1999.
- [8] J. Gegelia and G. Japaridze. Matching heavy particle approach to relativistic theory. *Phys. Rev. D*, 60:114038, 1999.
- [9] T. Fuchs, J. Gegelia, G. Japaridze, and S. Scherer. Renormalization of relativistic baryon chiral perturbation theory and power counting. *Phys. Rev. D*, 68:056005, 2003.
- [10] M. R. Schindler, T. Fuchs, J. Gegelia, and S. Scherer. Axial, induced pseudoscalar, and pion-nucleon form-factors in manifestly Lorentz-invariant chiral perturbation theory. *Phys. Rev. C*, 75:025202, 2007.
- [11] L. S. Geng, J. Martin Camalich, L. Alvarez-Ruso, and M. J. Vicente Vacas. Leading SU(3)-breaking corrections to the baryon magnetic moments in chiral perturbation theory. *Phys. Rev. Lett.*, 101:222002, 2008.
- [12] J. Martin Camalich, L. S. Geng, and M. J. Vicente Vacas. The lowest-lying baryon masses in covariant SU(3)-flavor chiral perturbation theory. *Phys. Rev. D*, 82:074504, 2010.
- [13] X. L. Ren, L. S. Geng, J. Martin Camalich, J. Meng, and H. Toki. Octet baryon masses in next-to-next-to-next-to-leading order covariant baryon chiral perturbation theory. *JHEP*, 12:073, 2012.
- [14] J. M. Alarcón, J. Martin Camalich, and J. A. Oller. The chiral representation of the πN scattering amplitude and the pion-nucleon sigma term. *Phys. Rev. D*, 85:051503, 2012.
- [15] J. M. Alarcón, J. Martin Camalich, and J. A. Oller. Improved description of the πN scattering phenomenology in covariant baryon chiral perturbation theory. *Annals Phys.*, 336:413–461, 2013. [Private communication with J.M. Alarcón].
- [16] Y.-H. Chen, D.-L. Yao, and H. Q. Zheng. Analyses of pion-nucleon elastic scattering amplitudes up to $\mathcal{O}(p^4)$ in extended-on-mass-shell subtraction scheme. *Phys. Rev. D*, 87:054019, 2013.
- [17] D.-L. Yao, D. Siemens, V. Bernard, E. Epelbaum, A. M. Gasparyan, J. Gegelia, H. Krebs, and U.-G. Meißner. Pion-nucleon scattering in covariant baryon chiral perturbation theory with explicit Delta resonances. *JHEP*, 05:038, 2016.
- [18] J.-X. Lu, L.-S. Geng, X.-L. Ren, and M.-L. Du. Meson-baryon scattering up to the next-to-next-to-leading order in covariant baryon chiral perturbation theory. *Phys. Rev. D*, 99(5):054024, 2019.
- [19] N. Fettes, U.-G. Meißner, and S. Steininger. Pion-nucleon scattering in chiral perturbation theory (I): Isospin symmetric case. *Nucl. Phys. A*, 640:199–234, 1998.
- [20] N. Fettes and U.-G. Meißner. Pion nucleon scattering in chiral perturbation theory (II): Fourth order calculation. *Nucl. Phys. A*, 676:311, 2000.
- [21] H. Krebs, A. Gasparyan, and E. Epelbaum. Chiral three-nucleon force at N4LO I: Longest-range contributions. *Phys. Rev. C*, 85:054006, 2012.
- [22] D. R. Entem, N. Kaiser, R. Machleidt, and Y. Nosyk. Peripheral nucleon-nucleon scattering at fifth order of chiral perturbation theory. *Phys. Rev. C*, 91(1):014002, 2015.
- [23] B.-L. Huang and Y.-D. Li. Kaon-nucleon scattering to one-loop order in heavy baryon chiral perturbation theory. *Phys. Rev. D*, 92(11):114033, 2015. [Erratum: *Phys. Rev. D*95,019903(2017)].
- [24] B.-L. Huang, J.-S. Zhang, Y.-D. Li, and N. Kaiser. Meson-baryon scattering to one-loop order in heavy baryon chiral perturbation theory. *Phys. Rev. D*, 96(11):016021, 2017.
- [25] N. Kaiser. Chiral corrections to kaon nucleon scattering lengths. *Phys. Rev. C*, 64:045204, 2001. [Erratum: *Phys. Rev. C*73,069902(2006)].

- [26] Y.-R. Liu and S.-L. Zhu. Meson-baryon scattering lengths in HB χ PT. *Phys. Rev. D*, 75:034003, 2007.
- [27] Y.-R. Liu and S.-L. Zhu. Decuplet contribution to the meson-baryon scattering lengths. *Eur. Phys. J. C*, 52:177–186, 2007.
- [28] Z.-W. Liu, Y.-R. Liu, and S.-L. Zhu. Pseudoscalar meson and decuplet baryon scattering lengths. *Phys. Rev. D*, 83:034004, 2011.
- [29] Z.-W. Liu and S.-L. Zhu. Pseudoscalar meson and charmed baryon scattering lengths. *Phys. Rev. D*, 86:034009, 2012. [Erratum: *Phys. Rev. D*93,no.1,019901(2016)].
- [30] B.-L. Huang and J. Ou-Yang. Pion-nucleon scattering to $\mathcal{O}(p^3)$ in heavy baryon SU(3) chiral perturbation theory. *Phys. Rev. D*, 101:056021, 2020.
- [31] S.-Z. Jiang, Q.-S. Chen, and Y.-R. Liu. Meson-baryon effective chiral Lagrangians at order p^4 . *Phys. Rev. D*, 95(1):014012, 2017.
- [32] J. Gasser and U.-G. Meißner. On the phase of epsilon-prime. *Phys. Lett. B*, 258:219–224, 1991.
- [33] T. E. O. Ericson and W. Weise. *Pions and nuclei*. Clarendon Press, Oxford, UK, 1988.
- [34] M. Tanabashi *et al.*. Review of Particle Physics. *Phys. Rev. D*, 98(10):030001, 2018.
- [35] C. C. Chang *et al.*. A per-cent-level determination of the nucleon axial coupling from quantum chromodynamics. *Nature*, 558:91–94, 2018.
- [36] B. Märkisch *et al.*. Measurement of the weak axial-vector coupling constant in the decay of free neutrons using a pulsed cold neutron beam. *Phys. Rev. Lett.*, 122:242501, 2019.
- [37] W. J. Briscoe *et al.*, SAID on-line program, see <http://gwdac.phys.gwu.edu>.
- [38] R. L. Workman, R. A. Arndt, W. J. Briscoe, M. W. Paris, and I. I. Strakovsky. Parameterization dependence of T matrix poles and eigenphases from a fit to πN elastic scattering data. *Phys. Rev. C*, 86:035202, 2012.
- [39] J. Dobaczewski, W. Nazarewicz, and P.-G. Reinhard. Error estimates of theoretical models: a Guide. *J. Phys. G*, 41:074001, 2014.
- [40] B. D. Carlsson *et al.*. Uncertainty analysis and order-by-order optimization of chiral nuclear interactions. *Phys. Rev. X*, 6(1):011019, 2016.
- [41] H. C. Schroder *et al.*. The pion nucleon scattering lengths from pionic hydrogen and deuterium. *Eur. Phys. J. C*, 21:473–488, 2001.
- [42] M. Hoferichter, J. Ruiz de Elvira, B. Kubis, and U.-G. Meißner. High-precision determination of the pion-nucleon σ -term from Roy-Steiner equations. *Phys. Rev. Lett.*, 115:092301, 2015.